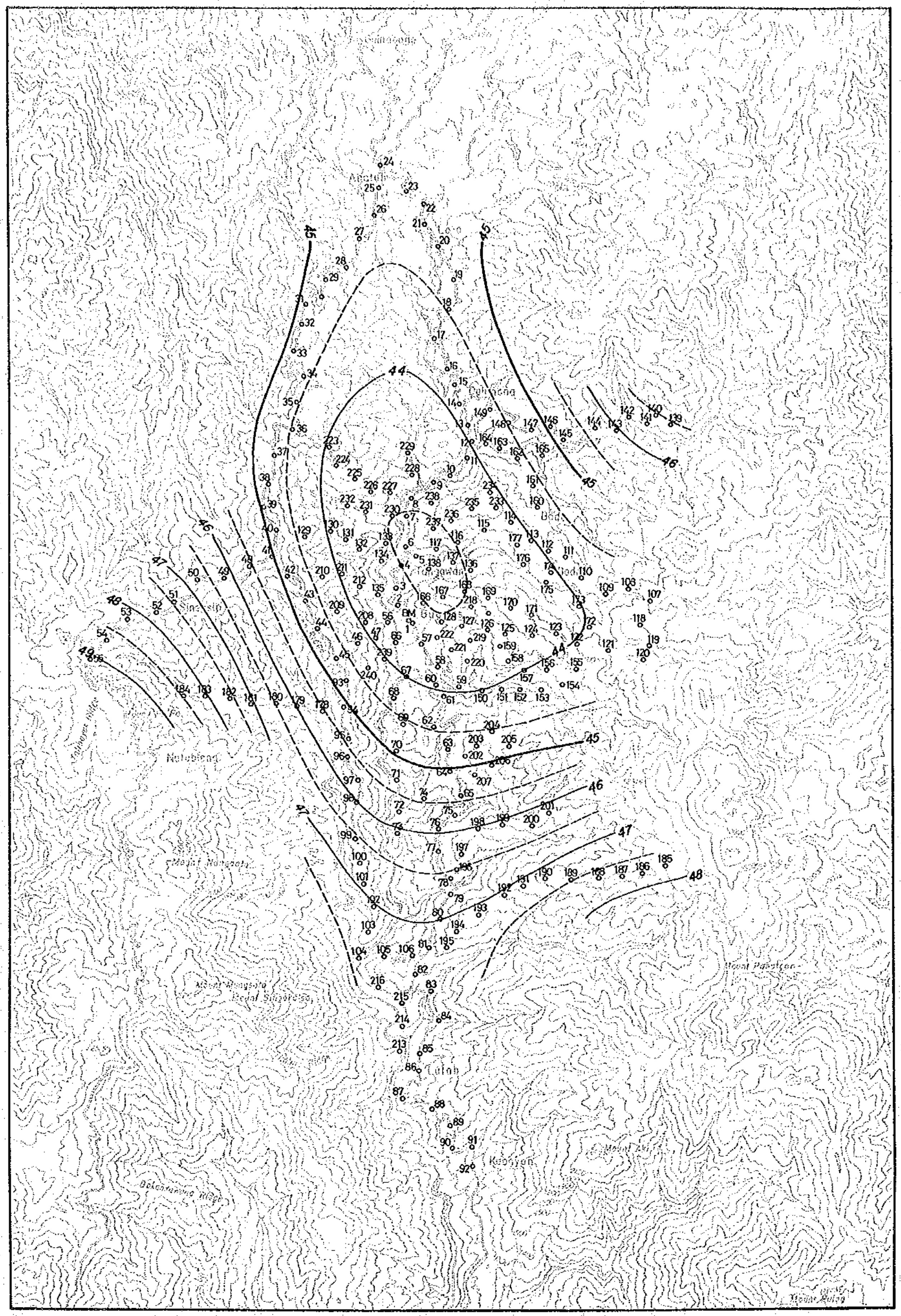

Buguias Geothermal Development Survey
the Republic of the Philippines

RESIDUAL GRAVITY MAP
(λ = 9.5)

0 1000 6000 km

Jan ~ Feb, 1981

Fig. II -3-12

of them show the reverse coincidense which could be explained by the lower density layer in the depth lacking the overburden with higher density.

W

52
50
48
46
44
42
40
38

Bouguer
Regional
Residual (λ=1.8~9.5)
Residual (λ=0.25~1.8)

2
1
0
-1
-2

2
1
0
-1
-2

Sinepsip
52
Pulibo Ridge
172
208
Agno River
1
Buguias
127

2000 m
1000
0

2.5±0.1
2.6 ± 0.05
2.7 ± 0.05

E

52
50
48
46
44
42
40
38

2
1
0
-1
-2

Pulibo Ridge

208

Agno River

Buguias

1

127

172

2000 m

1000

0

2.5±0.1

2.6 ± 0.05

2.7 ± 0.05

Buguias Geothermal Development Survey
the Republic of the Philippines

CROSS SECTION (E-W) AND STRUCTURAL MODEL

0 500 1000 m

Jan~Feb, 1981

Fig. Ⅱ-3-13

CHAPTER 4 MAGNETIC SURVEY

Chapter 4

Magnetic Survey

4–1 Objective of Survey

Magnetic survey for geothermal fields is usually conducted for the purpose of clarifying the geological structures and/or detecting the slight change of demagnetization due to the geothermal alteration. General geological structures are studied by airborne magnetic survey which measures wide geomagnetic change, while geothermal demagnetization is usually detected by ground magnetic survey.

A magnetic anomaly is mainly caused by the igneous rocks such as basalt and andesite in which the strong magnetizing minerals, mostly magnetite are contained. This anomaly is known as induced magnetization which is caused by the present geomagnetic field. On the other hand remanent magnetization, which is known as paleo-magnetism induced under the cooling process in the past magnetic field must also be studied.

Around a known geothermal resource area, high temperature geothermal fluids exist at depths are characterized by regional low magnetic anomalies known as demagnetization due to geothermal alteration.

In this survey, those phenomena were studied by means of a high accuracy magnetometer and relations between geological structures and geothermal effects are discussed.

4–2 Method of Survey

4–2–1 Abstract

The earth's magnetic field resembles the field of a large magnetic bar near its center or that due to a uniformly magnetized sphere. The direction of the field is vertical at the north and south magnetic poles, and horizontal at the magnetic equator. The intensity of the field, which is a function of the density of the 'flux lines' shown below, again behaves as a bar magnet being twice as large in the polar region as in the equatorial region, or approxi-

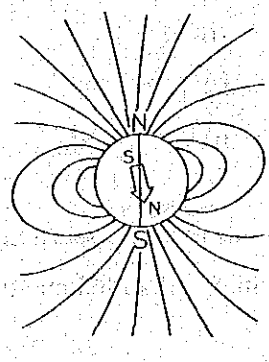

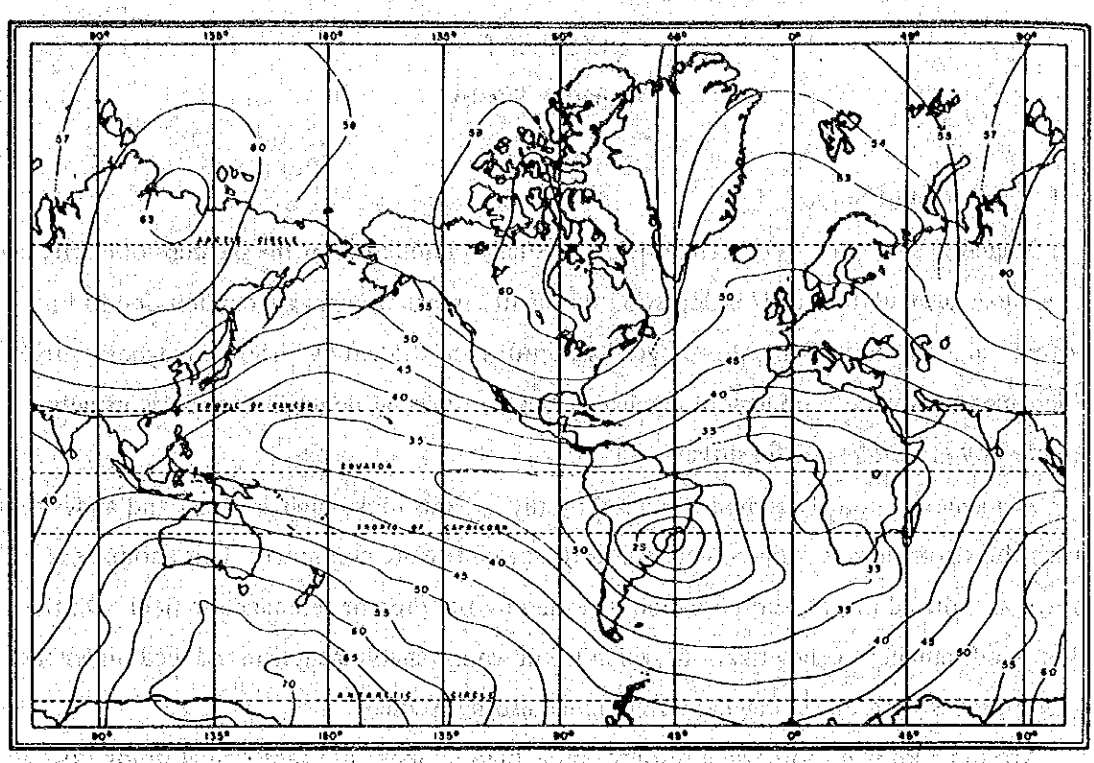

Fig. II–4–1 Total Intensity of the Geomagnetic Field

mately 60,000γ (gammas) in Northern Canada and about 40,000γ in Luzon Island respectively. The total intensity is shown in Fig. II–4–1. The earth cannot exactly be represented by a single bar magnet, but has numerous higher order poles and very large-scale anomalous features owing to unknown characteristics of the generating mechanism in the earth's core.

Typical susceptibilities of rocks are given below, but may vary by an order of magnitude or more in most cases:

Granite	$10^{-5} \sim 10^{-3}$
Andesite	10^{-4}
Rhyolite	$10^{-5} \sim 10^{-4}$
Shale	$10^{-5} \sim 10^{-4}$
Metamorphic rocks	$10^{-4} \sim 10^{-6}$
Sedimentary rocks	$10^{-6} \sim 10^{-5}$
Limestone-chert	10^{-6}

Typically, dark, more basic igneous rocks possess a higher susceptibility than the acidic igneous rocks and the latter, in turn, higher than sedimentary rocks.

The remanent magnetization of a rock or object may or may not be in the same direction as the present earth's field for the object may be reoriented because the earth's field is known to have changed its orientation in geologic and even historic time. The direction of remanent magnetization is not constant, but it does not affect so much the magnetic structure interpretation.

Total Field Measurement

The total magnetic field intensity, as measured by a proton magnetometer, is a scalar measurement, or simply the magnitude of the earth's field vector independent of its direction.

The total field intensity is very significant with respect to the asymmetric signatures of anomalies, interpretation of anomalies, and in various special applications.

The depth, shape and the susceptibility difference can be determined by the shape of an anomaly, amplitude and wave-length.

Anomalies of very short wave-lengths are presently caused by the magnetic materials.

A 5 point running average was adopted on each observed value for every 50 m interval. The average values are then plotted on the plain and section maps.

4–2–2 Survey Lines and Stations

In order to confirm the general geomagnetic structure of the survey area 3 ~ 4 stations were planned on and between the gravity stations in the area of 12 Km in E-W and 15 Km in N-S with Buguias village as its center. Station intervals were measured by pace and it is around 150 m confirming the location at the gravity station. A magnetic base station was settled in Buguias village and two readings were made on the base station at the beginning and at the end of the survey. Those readings together with the base magnetic recording were used to check the diurnal change. The stations are numbered consecutively from one to 1,000, as shown in the location map of magnetic survey station on Fig. II–4–2.

4–2–3 Magnetometer

The Proton magnetometers used in the survey are as follows:

Portable proton magnetometer G-816 made by Geometrics, USA (2 sets)
GM-122 made by Barringer Research, Canada

Resolution . . .	± 1 γ (Digital display)
Tuning Range . .	20,000 ~ 100,000 γ (Worldwide)
Gradient Tolerance . . .	150 γ/feet (1900 γ/m for GM-122)

The GM-122 Proton magnetometer was one of the equipment given to the Philippine Government from the Japanese Government.

The observation crew consisted of one staff man, one observer and one recording man.

As a result of comparison measurements of the G-816 and GM-122, it becomes clear that the deviation are only due to the staff height differences so that GM-122 was used for this survey.

Base magnetic recording system is designed by Bishimetal Exploration Co., LTD. as shown below.

Type	Base recording system
Sampling time	1, 2, 5, 10 minutes
Output	6 digital display and printing with 10 mV analog outlet

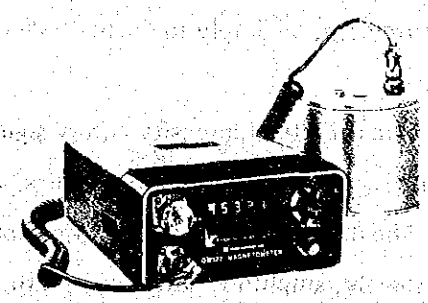

Theory

It has been some time since the nuclear magnetic resonance (NMR) type of magnetometer was used to measure the geomagnetic field. In recent years, the measuring instruments have been widely used on rugged topography with efficiency due to miniaturization and digital read-out system.

The nuclear magnetic resonance type magnetometer utilizes the magnetic gyration characteristics of the hydrogen nucleus (proton). By measuring the frequency of free precession of the proton in the geomagnetic field, it is possible to measure the strength of the geomagnetic field.

As proton is in abundant existence in water, kerosene and alcohol, these liquids may be sealed in a container surrounded by a coil (pick up and polarizing coil). When the polarizing field is momentarily applied and is stronger than the geomagnetic field, the protons will line up in the direction of the polarizing field. When the polarizing field is suddenly cut off, the protons will process like a spinning top about the direction of the geomagnetic field. In this case, the free-precession frequency, f, is proportional to the geomagnetic field strength Ho, so that

$$Ho = 2\pi f/\gamma$$

In the above equation, y is called the gyromagnetic ratio (magnetic moment/spin angular momentum) of the proton. It is a physical constant depending on the types of nuclei and its value for the proton is $0.267528 \pm 0.00006 \times 10^4$ sec^{-1} $gauss^{-1}$.

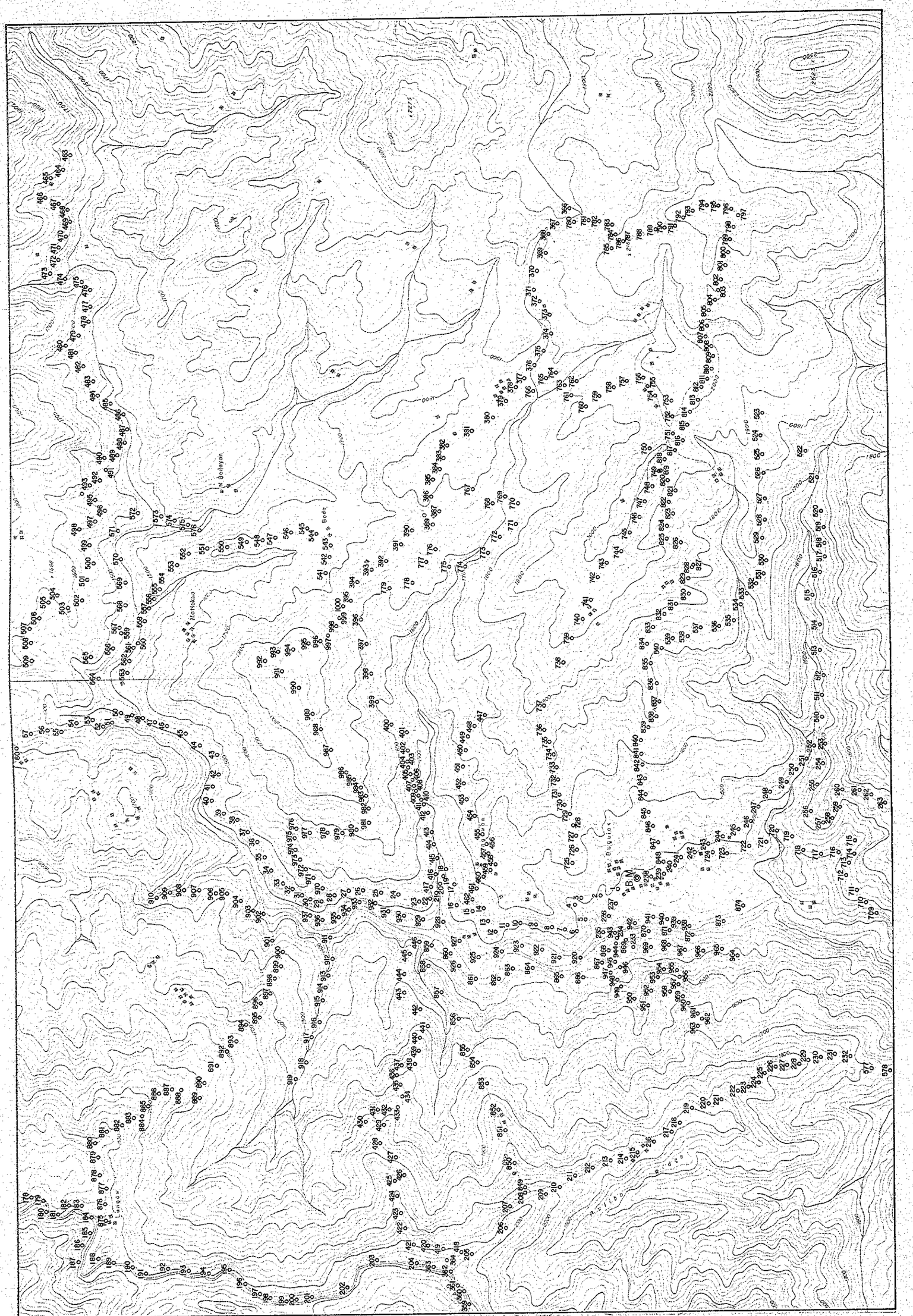

Buguias Geothermal Development Survey
the Republic of the Philippines

LOCATION OF MAGNTIC STATION

0 500 1500m

Jan~Feb, 1981

Fig. II-4-2

In the above mentioned manner, by using the same polarizing coil, it is possible to measure the frequency, which is proportional to the strength of the geomagnetic field, and to read the geomagnetic force in gamma directly from the digital display.

4–2–4 Magnetic Correction

Intensity of geomagnetic field is not always constant. It has a periodical change and its frequency changes from several seconds, known as micro pulsations, up to several hours such as magnetic storms which are considered to be mainly caused by electric current in the E-ionosphere, or above 100 Km from the ground.

Those magnetic changes are originally affected by magnetic changes on the solar surface, and are consequently deeply related with the positions of the sun and the earth. The solar surface is reported to be active every 11 years and this year, 1981, fits the peak of the activity, so that it is very important to watch the diurnal change at the base station.

Every diurnal change monitored at the base station during the survey period from January 31, 1981 to March 4, 1981 are shown in Fig. II–4–3.

4–3 Method of Analysis and Interpretation

4–3–1 Susceptibility Measurements

In order to analyze the magnetic structures which cause anomalies and magnetic susceptibilities, the depth and the shape should be determined. Collected rock samples were measured by the following procedure.

Special care has been taken to avoid iron particles of the hammer from mixing with the samples and an agate mortar was used to grid the samples down to –80 mesh. Sixty

grams of the power sample was put into a plastic tubular container (1" Dia. x 3" Long) and measured by the following instrument:

Bison Magnetic Susceptibility Meter 3101A

Range of measurement $1 - 100{,}000 \times 10^{6}$ e.m.u./cc

Bulk susceptibility is given as

$$K = R \cdot X \left(\frac{d}{d'}\right)^2 \cdot \left(\frac{\sigma}{\sigma'}\right) \cdot f \times 10^{-6}$$

R: Reading by BISON 3101A

d/d' : $\dfrac{\text{Diameter of standard sample (1 inch)}}{\text{Diameter of sample}}$

σ/σ' : $\dfrac{\text{Rock density}}{\text{Powdered density}}$

f : Coil constant = 1.00

4–3–2 Model

Since the measured geomagnetic force is a potential quartz, an indefinite number of models of a magnetic body can give a reasonable explanation to the results of the measurement.

It is therefore, necessary to determine which particular model is the most appropriate to the geological structure present in the surveyed area.

Quantitative interpretation of magnetic anomalies is usually done simply with models of magnetic rocks of sphere, cylinder, prism, step or dyke-structures, or a combination of these shapes.

In the area of low degree magnetic inclination (20°), like in this case, the results of magnetic survey is dominated with magnetic anomalies. Since its contour pattern has the tendency to the elongated in the east and west directions, even for spherically symmetric magnetic rocks, it is difficult to estimate the east and the west directions of the magnetic rock which have induced the observed anomalies.

It is very important to note in this field that magnetic anomalies are normally observed above high susceptibility rocks. Positive anomalies localized on the contour map or cross-section implies the existence of lower susceptibility rocks which are of high interest, as in the case of a geothermal region in relation to demagnetization phenomena.

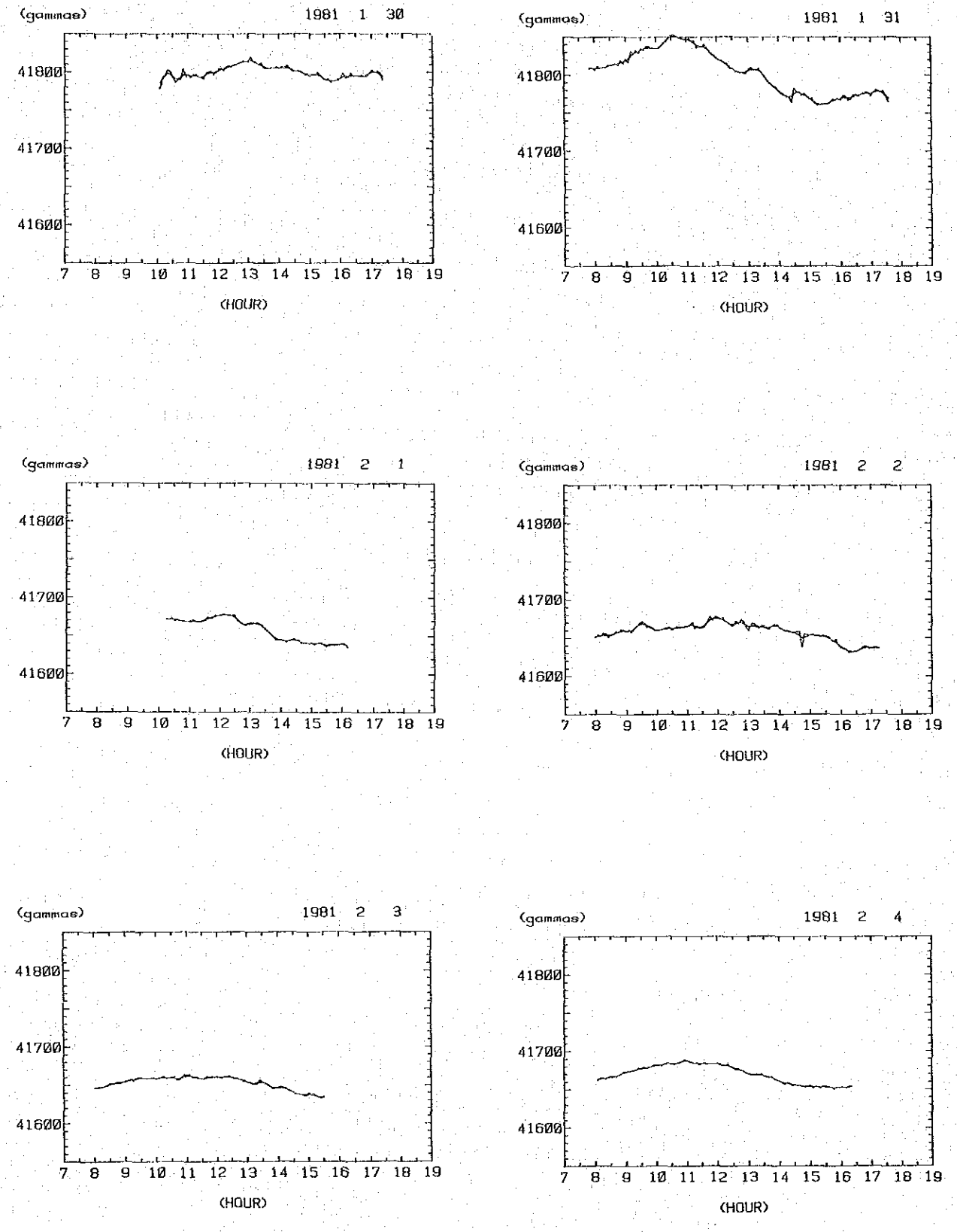

Fig. II–4–3 Diurnal Variation at Magnetic Station

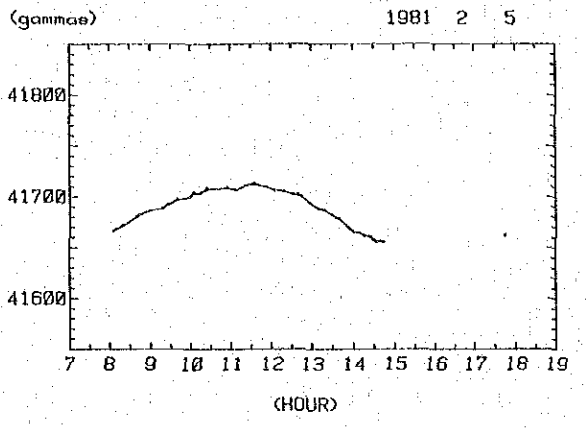
(gammas)
1981 2 5
41800
41700
41600
7 8 9 10 11 12 13 14 15 16 17 18 19
(HOUR)

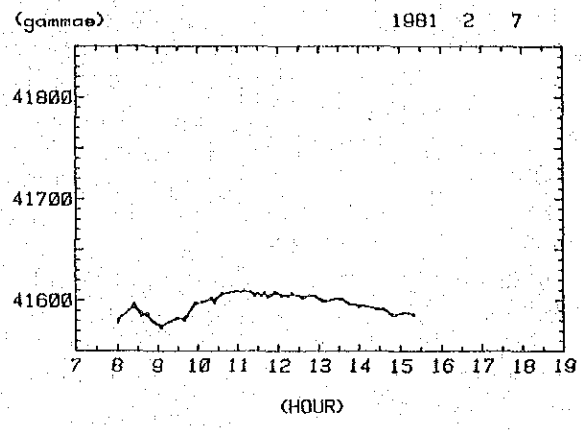
(gammas)
1981 2 7
41800
41700
41600
7 8 9 10 11 12 13 14 15 16 17 18 19
(HOUR)

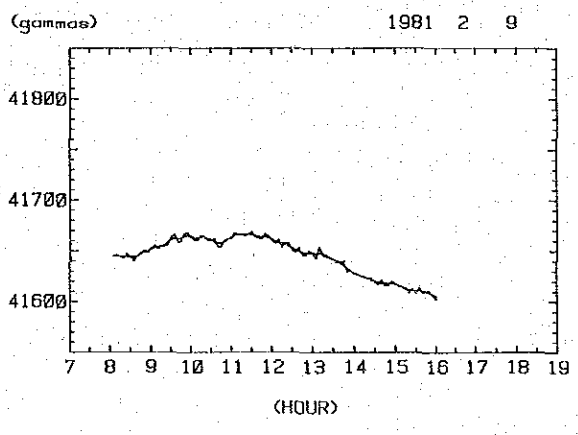
(gammas)
1981 2 9
41800
41700
41600
7 8 9 10 11 12 13 14 15 16 17 18 19
(HOUR)

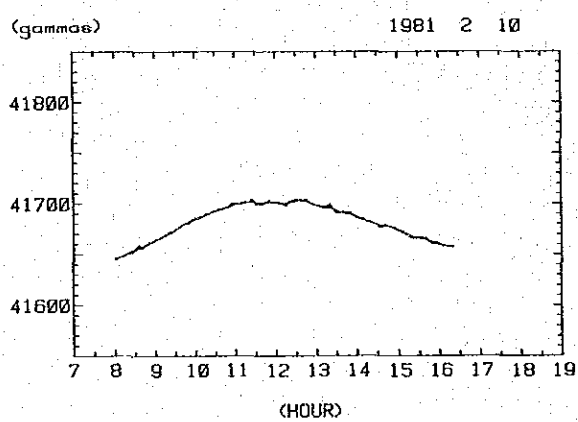
(gammas)
1981 2 10
41800
41700
41600
7 8 9 10 11 12 13 14 15 16 17 18 19
(HOUR)

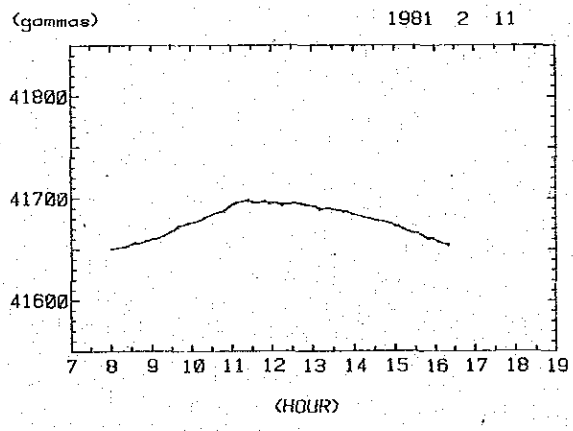
(gammas)
1981 2 11
41800
41700
41600
7 8 9 10 11 12 13 14 15 16 17 18 19
(HOUR)

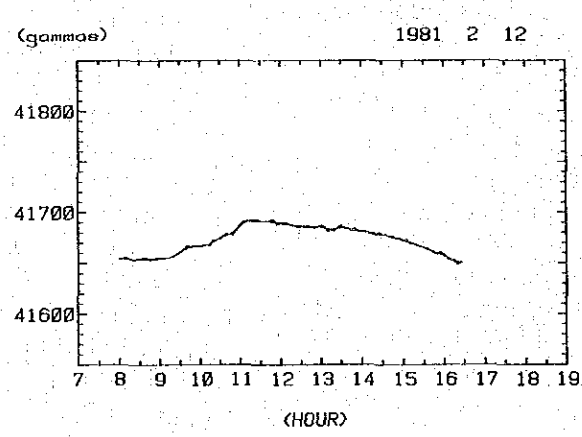
(gammas)
1981 2 12
41800
41700
41600
7 8 9 10 11 12 13 14 15 16 17 18 19
(HOUR)

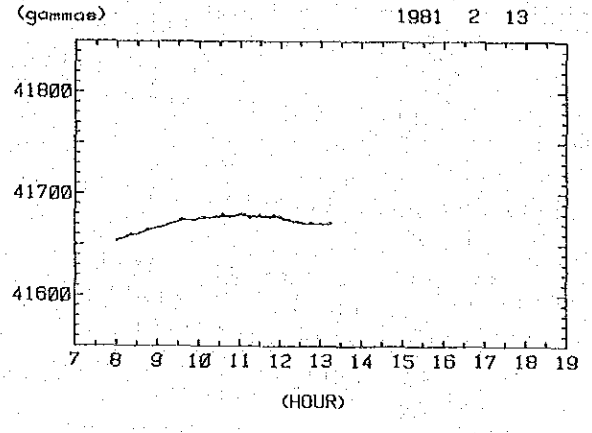
(gammas)
1981 2 13
41800
41700
41600
7 8 9 10 11 12 13 14 15 16 17 18 19
(HOUR)

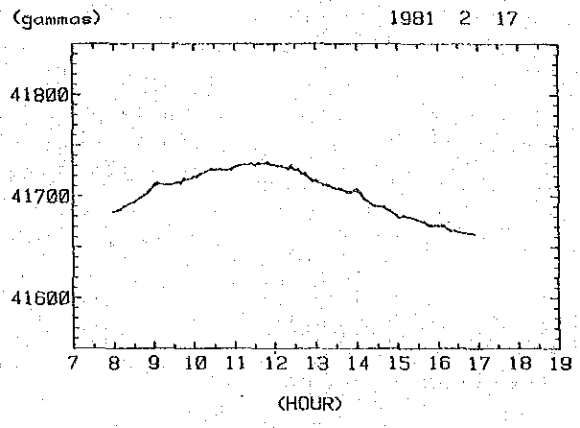
(gammas)
1981 2 17
41800
41700
41600
7 8 9 10 11 12 13 14 15 16 17 18 19
(HOUR)

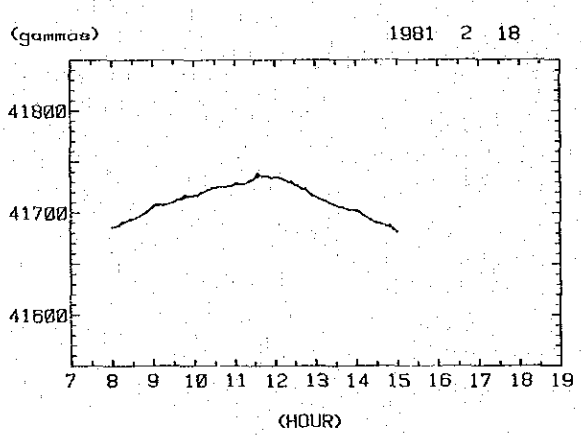
(gammas)
1981 2 18
41800
41700
41600
7 8 9 10 11 12 13 14 15 16 17 18 19
(HOUR)

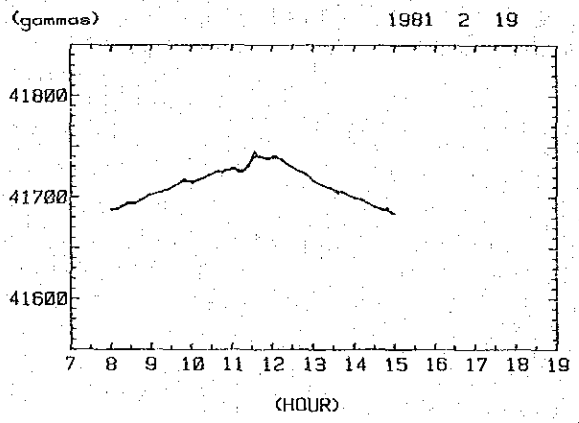
(gammas)
1981 2 19
41800
41700
41600
7 8 9 10 11 12 13 14 15 16 17 18 19
(HOUR)

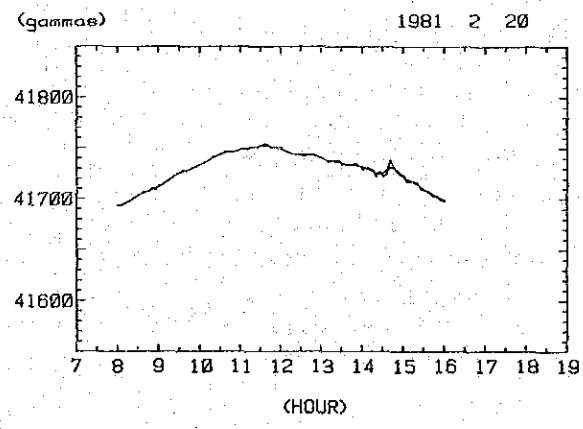
(gammas)
1981 2 20
41800
41700
41600
7 8 9 10 11 12 13 14 15 16 17 18 19
(HOUR)

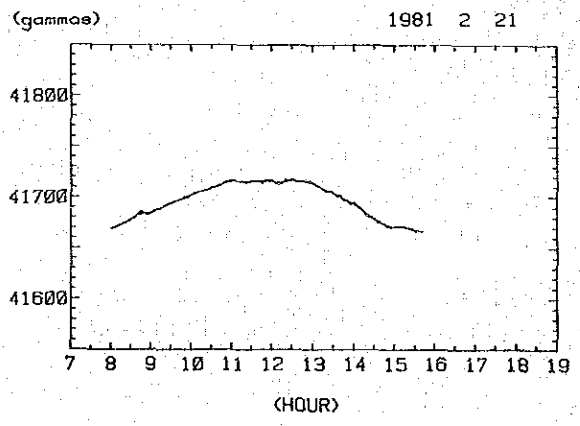
(gammas)
1981 2 21
41800
41700
41600
7 8 9 10 11 12 13 14 15 16 17 18 19
(HOUR)

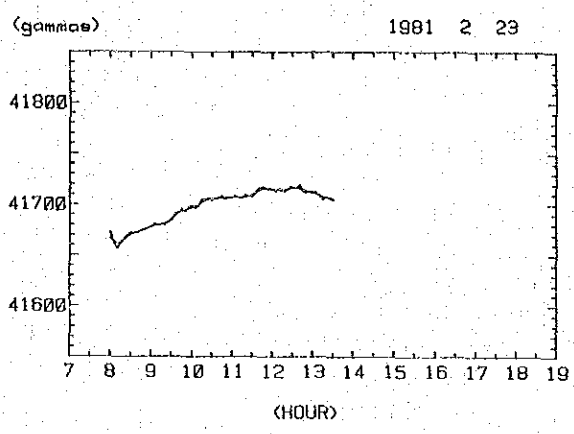
(gammas)
1981 2 23
41800
41700
41600
7 8 9 10 11 12 13 14 15 16 17 18 19
(HOUR)

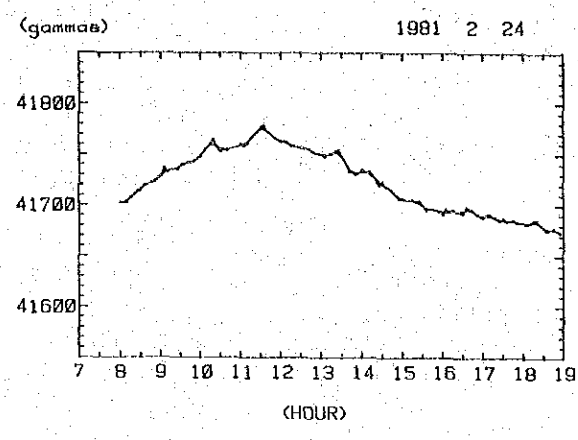
(gammas)
1981 2 24
41800
41700
41600
7 8 9 10 11 12 13 14 15 16 17 18 19
(HOUR)

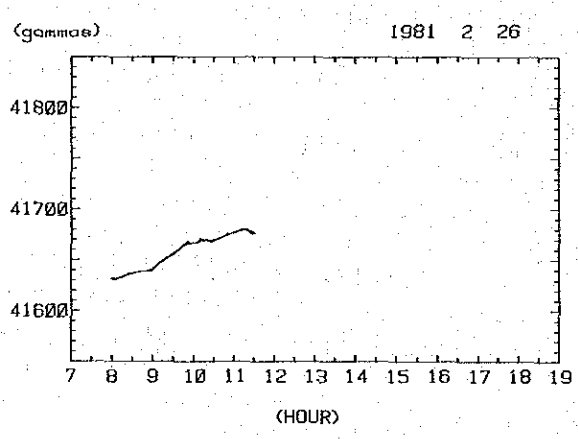
(gammas)
1981 2 26
41800
41700
41600
7 8 9 10 11 12 13 14 15 16 17 18 19
(HOUR)

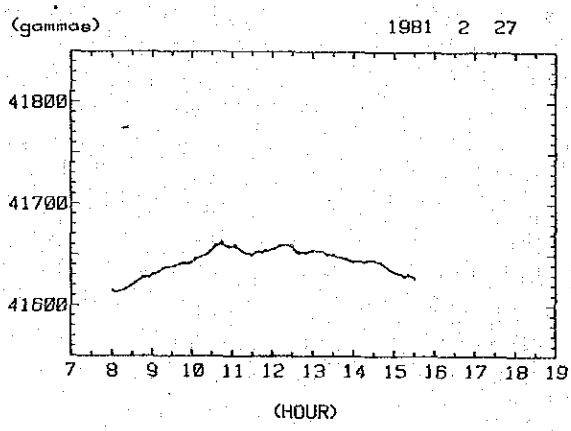
(gammas)
1981 2 27
41800
41700
41600
7 8 9 10 11 12 13 14 15 16 17 18 19
(HOUR)

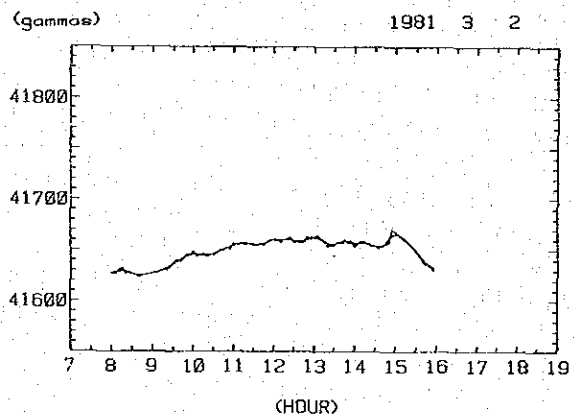
(gammas)
1981 3 2
41800
41700
41600
7 8 9 10 11 12 13 14 15 16 17 18 19
(HOUR)

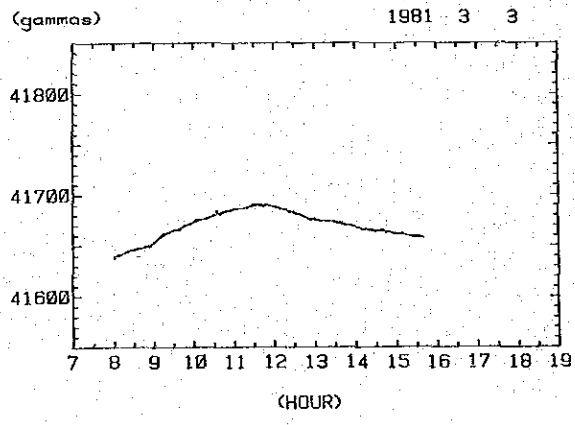
(gammas)
1981 3 3
41800
41700
41600
7 8 9 10 11 12 13 14 15 16 17 18 19
(HOUR)

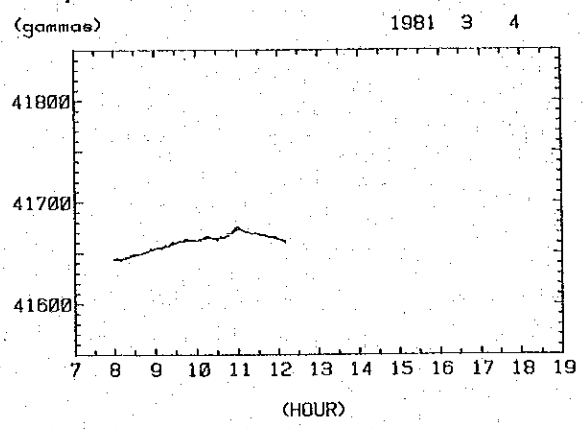
(gammas)
1981 3 4
41800
41700
41600
7 8 9 10 11 12 13 14 15 16 17 18 19
(HOUR)

Table II–4–1 Magnetic Susceptibility

Serial No.	Sample No.	Case No.	Wo (g)	W (g)	W′ (g)	σ′ (g/cc)	σ (g/cc)	σ / σ′	Multi-plication	Reading R	X (e.m. u/g)	k (e.m. u/cc)	Rock Facies
1	M–17	1	6032	11962	5930	1,91	2,75	1.44	1	2272		3276	andesitic pillow lava
2	19	2	6043	11802	5759	1.85	2.80	1.51		1010		1527	andesite dyke
3	37	3	6062	11349	5287	1.70	2.37	1.39		514		716	andesitic pillow lava
4	42	4	6048	11628	5580	1.79	2.47	1.38		47		65	fine - coarse tuff
5	57	5	6054	11598	5544	1.78	2.60	1.46		3286		4792	andesite dyke
6	61	6	6052	12030	5978	1.92	2.66	1.38		4782		6617	hb-andesite
7	74	7	6050	11959	5909	1.90	2.58	1.36		2456		3335	hb-andesite
8	N–10	8	6060	12104	6044	1.94	2.55	1.31	1	2585		3391	qtz-diorite
9	11	9	6040	12323	6283	2.02	2.67	1.32		7596		10038	brecciated andesite
10	12	10	6062	11992	5930	1.91	2.59	1.36		2070		2811	hb-andesite
11	15	1	6032	11502	5470	1.76	2.47	1.40		1342		1884	hb-qtz-diorite
12	26	2	6043	11561	5518	1.77	2.66	1.50		3120		4677	andesite
13	33	3	6062	12018	5956	1.92	2.60	1.36		2406		3266	px-hb-andesite
14	39	4	6048	11520	5472	1.76	2.50	1.42		1288		1830	hb-andesite
15	76	5	6054	11379	5325	1.71	2.63	1.54		2956		4540	hb-andesite
16	79	6	6052	10515	4463	1.44	2.39	1.67		46		77	altered-rhyolite
17	83	7	6050	11058	5008	1.61	2.32	1.44		936		1348	tuff breccia
18	N–113	8	6060	11840	5780	1.86	2.44	1.31	1	1166		1531	hb-dacite
19	115	9	6040	11419	5379	1.73	2.60	1.50		3544		5329	hb-andesite
20	118	10	6062	11606	5544	1.78	2.52	1.41		1946		2751	hb-andesitic porphyry
21	134	1	6032	11166	5134	1.65	2.53	1.53		1614		2473	hb-andesitic tuff breccia
22	142b	5	6054	11086	5032	1.62	2.51	1.55		224		347	tuffaceous limestone
23	156	2	6043	10919	4876	1.57	2.56	1.63		1414		2309	andesite brecciated lava
24	161	3	6062	11397	5335	1.72	2.50	1.46		585		852	basic andesite
25	165	4	6048	11216	5168	1.67	2.43	1.46		786		1145	tuff breccia

Fig. II–4–4 shows the results of the calculation for dyke models with inclination 20°. Strike angle is taken in the direction of the magnetic north. Magnetic anomaly due to a dyke model is given as

$$T_D(y, o) = \Delta K \cdot To\,(1 - \cos^2 I \sin^2 D) \sin d \left\{ \cos(2i - d - \frac{\pi}{2}) \left(\tan^{-1} \frac{y + \frac{w}{2}}{z} - \tan^{-1} \frac{y - \frac{w}{2}}{z}\right) + \sin(2i - d - \frac{\pi}{2}) \ln \frac{(y + \frac{w}{2})^2 + z^2}{(y - \frac{w}{2})^2 + z^2} \right\}$$

where,

y : y-axis is taken in the direction at an angle of D (=90°−θ) to the magnetic north, i.e. the direction perpendicular to the trend of the dyke structure,

z : z-axis is taken vertically downward to the upper surface of the dyke structure,

w : Width of the dyke structure,

$\Delta K = K_1 - K_2$: Difference of susceptibility between inside and outside the dyke,

To : Intensity of geomagnetic field,

I : Inclination of geomagnetic field,

d : Dip of the dyke,

i ; $\tan^{-1}$ (tan I/cos D) Apparent inclination

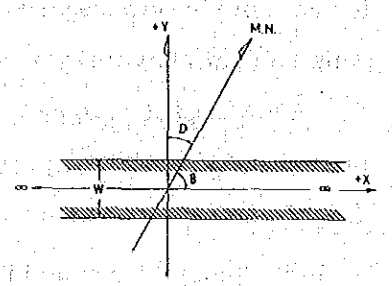

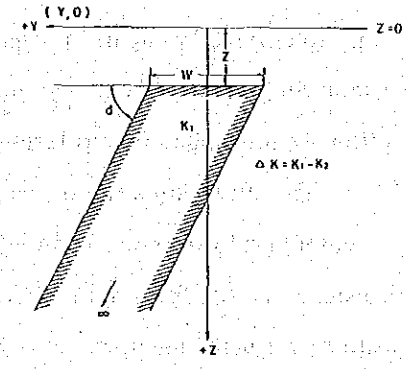

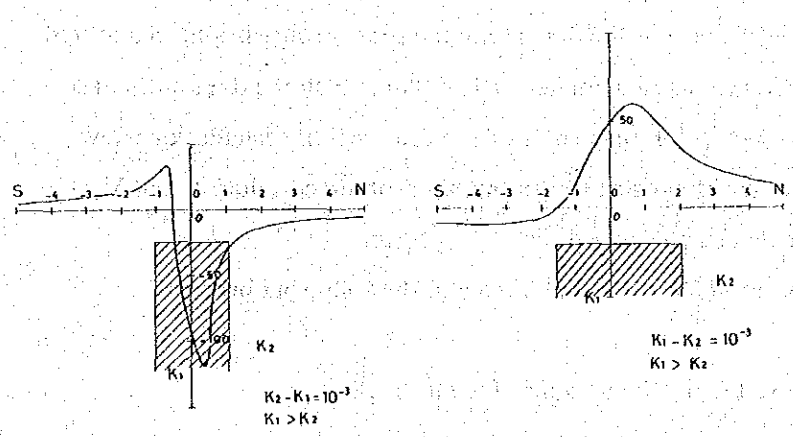

Fig. II–4–4 Magnetic Anomaly Caused by Dyke

4–3–3 Interpretation on Iso-Gamma Map

Magnetic anomaly (γ_o) is calculated by subtracting the diurnal change of the observation day ($\Delta\gamma_d$) and the mean value of the total data ($\bar{\gamma}$) from the observed total magnetic intensity ($\Delta\gamma$) at each station:

$$\Delta\gamma = \gamma_o - \Delta\gamma_d - \bar{\gamma}$$

where, average of the total data is 40961γ in this field.

This anomaly include the regional geological noise, topographic and cultural effects with comparatively short wave lengths. The raw iso-gamma map is shown in Fig. II–4–5. It is difficult to draw a contour line for each data because of the sudden changes due to the short wave anomalies, that only the general trends of the anomalies are enclosed.

Judging from this pattern, a wide E-W stretching high magnetic anomaly is seen in the north of Toking creek. The model calculation indicates a high magnetic anomaly which is seen above the low-magnetic susceptibility rocks. In this area, comparatively low-magnetized sedimentary rocks are widely distributed in the north of the E-W fault-like structure.

A low-magnetic anomaly widely covers Buguias Central stretching eastwards towards Bodoan and Ifugao province. This may correspond with the thermally altered zone coming down from the eastern mountains.

4–3–4 Interpretation on Filtered Map

In order to remove the disturbances of shallow geological and topographical effects and to emphasize the deep magnetic anomaly, some filtering has been applied on the raw data. In most cases, equi-gamma maps are divided into grids and the data on the intersection are multiplied by a filtering constant to get the filtered value.

The survey area is, however, mountainous, and as the desity is not good enough to conduct grid filtering, a running average of the data along the survey route has been adopted instead. A disc for a running average has a diameter of 1,000 m and all the data in the disc are used for the mean which is plotted on the center of the disc. All the calculations have been done by a desk-top computer by putting station number, observed value, X and Y coordinates, and then the calculated values are drawn by a plotter.

Consequently, small scale anomalies are eliminated and the following big scale anomalies come out:

(1) Low magnetic anomaly located north and along Toking creek

High magnetized rock

(2) Low magnetic belt extending E-W with (1) as its center

High magnetized rock

(3) Low magnetic anomaly in the upstream of Buguias creek

High magnetized rock

(4) A weak high magnetic anomaly extending eastwards from Buguias Central

Low magnetized rock

(5) High magnetic anomaly extending in E-W from north Dalimona

Low magnetized rock

High magnetized rock (1) may be due to andesitic - basaltic rocks of Loo formation widely distributed north of Toking creek, and sediments of iron sand can be seen on the surface.

Anomaly (2) is considered to be due to the combined effect of andesitic intrusive rocks outcropped along the N-W trending weak zone in the east of Pulibo ridge and along the E-W trending zone from Toking creek to Harshima road.

Anomaly (3) coincides well with the distribution of andesite - hornblende andesite porphyry.

Anomaly (4) is not clear, but the center is east of the Buguias Central and widely spread poorly-magnetized zones are confirmed.

This anomaly is due to comparatively the weakly magnetized Buguias formation affected by geothermal alteration which brought hot springs to the Buguias Central. As this anomaly extends eastwards towards Bodoan, this zone and its extension sound promising for the future exploration in the depths.

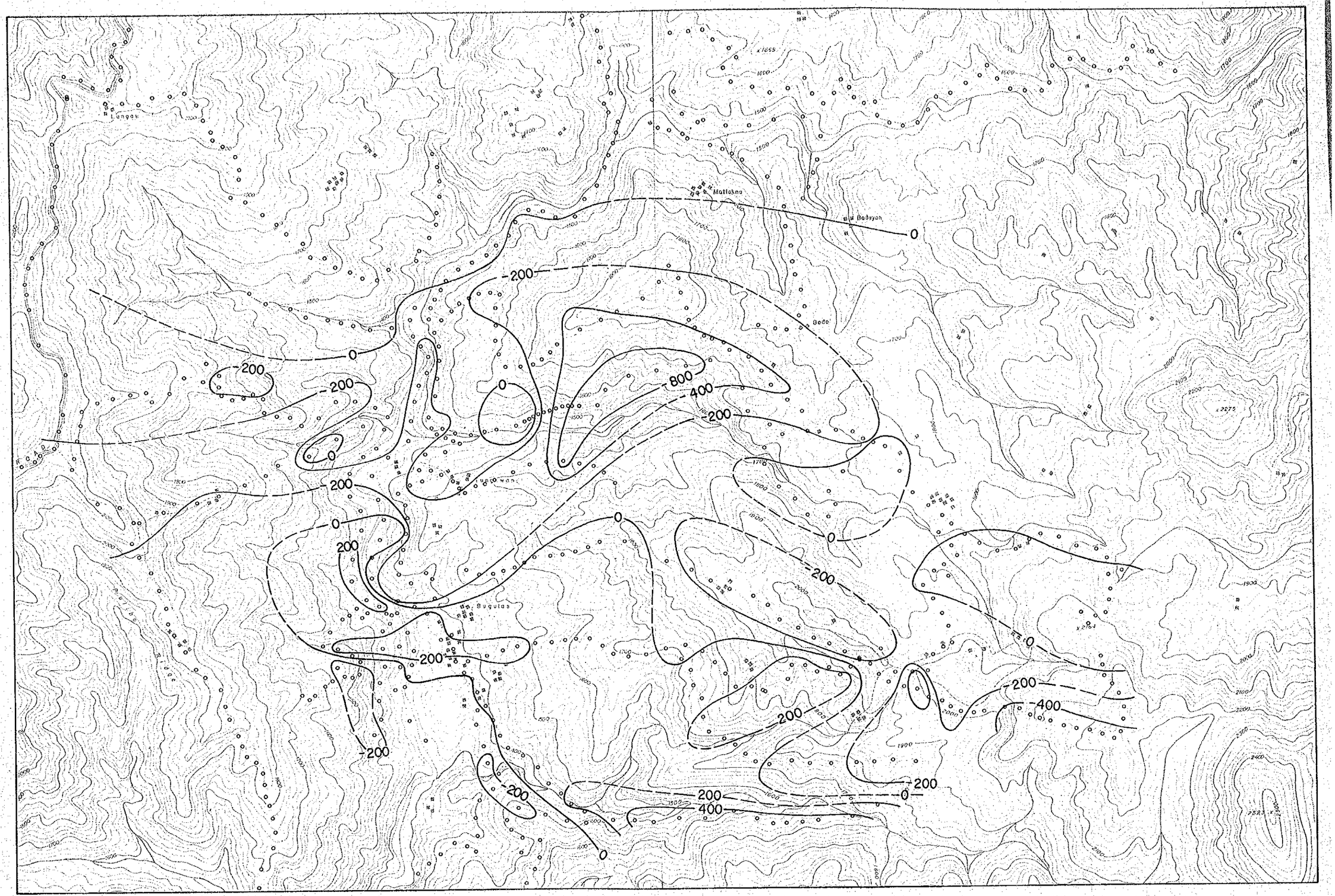
Lungsi
Matlakna
Babayan
Gedo
Sugutas
0
200
400
800

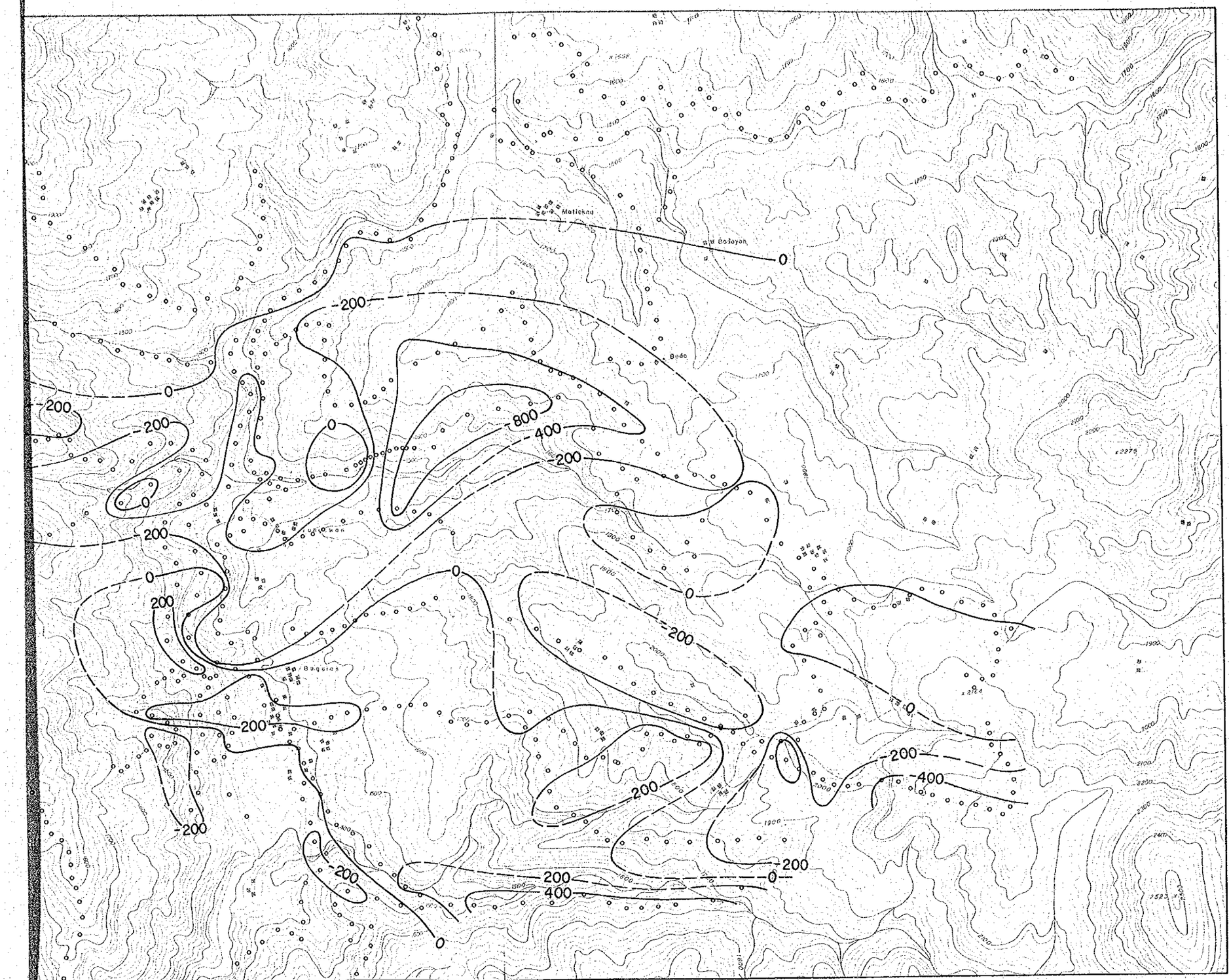

Bugulos Geothermal Development Survey
the Republic of the Philippines

OBSERVED MAGNETIC MAP

0 500 1500 m

Jan~Feb, 1981

Fig. II-4-5

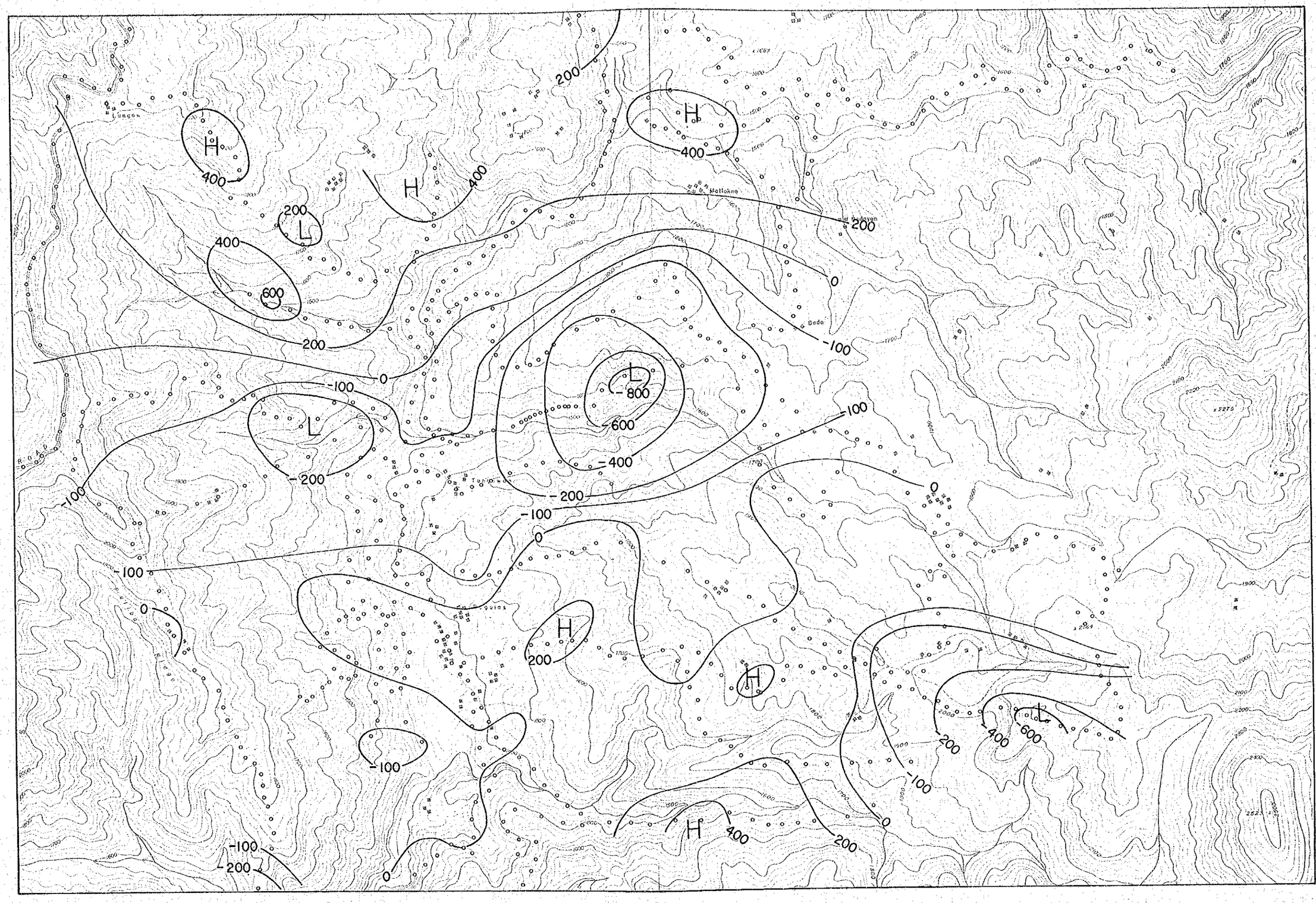
H
400
200
L
600
0
-100
-800
-400
-200
Lingon
Matloano
Dodo

Buguias Geothermal Development Survey
the Republic of the Philippines

FILTERED MAGNETIC MAP

0 500 1500 m

Jan ~ Feb, 1981

Fig. II-4-6

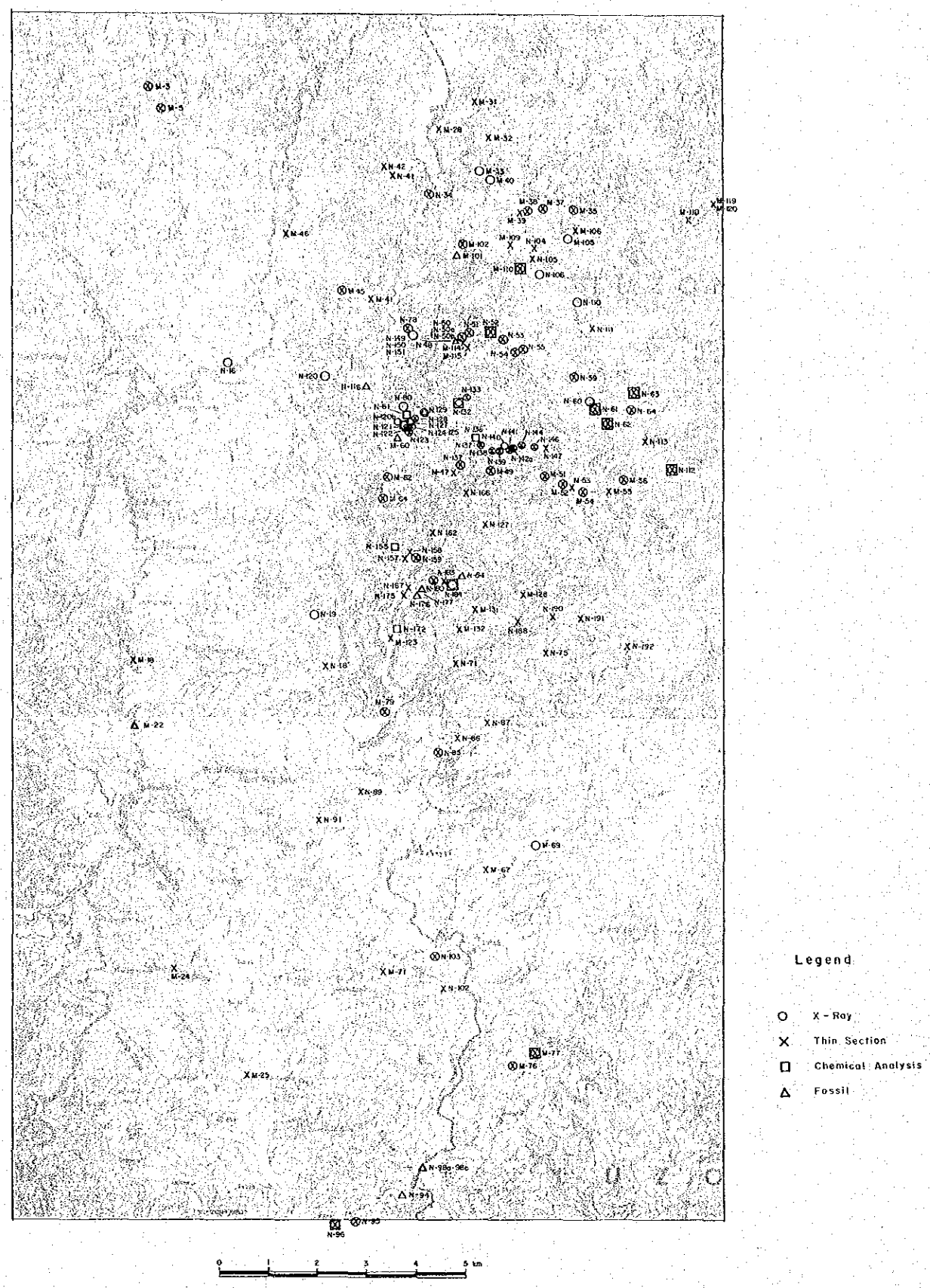

Fig. II-1-32 Location Map of Sample